AD-A192 137 ROUGHNESS EFFECTS ON ITTC (INTERNATIONAL TOWING TANK CONFERENCE) PROPELLE (U) DAVID W TAYLOR NAVAL SHIP RESEARCH AND DEVELOPMENT CENTER BET... Y T SHEN ET AL 1/1

UNCLASSIFIED JAN 88 DTNSRDC/SHD-1255-01 F/G 13/10 NL

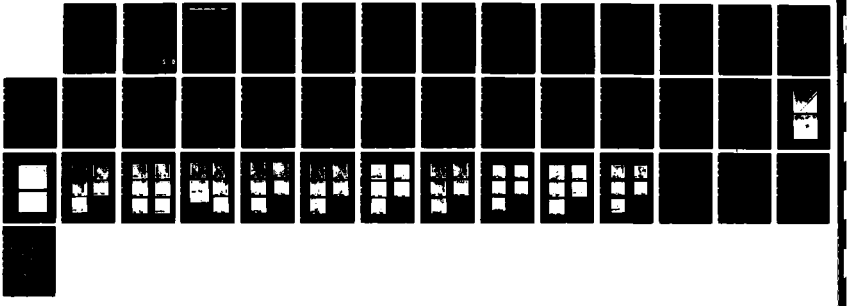

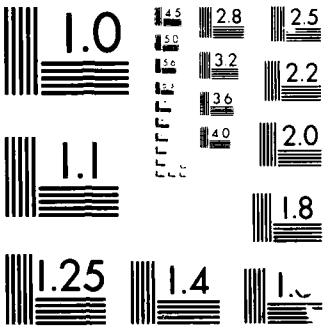

MICROCOPY RESOLUTION TEST CHART

AD-A192 137

DTIC FILE COPY

David W. Taylor Naval Ship Research and Development Center

Bethesda, MD 20084-5000

DTRC-SHD 1255-01 January 1988

Ship Hydromechanics Department

ROUGHNESS EFFECTS ON ITTC PROPELLER CAVITATION

by

Young T. Shen
Kirk J. Anderson

Approved for public release;
Distribution is unlimited.

DTIC
ELECTE
S MAR 1 1 1988 D
H

DTRC-SHD 1255-01 Roughness Effects on ITTC Propeller Cavitation

MAJOR DTNSRDC TECHNICAL COMPONENTS

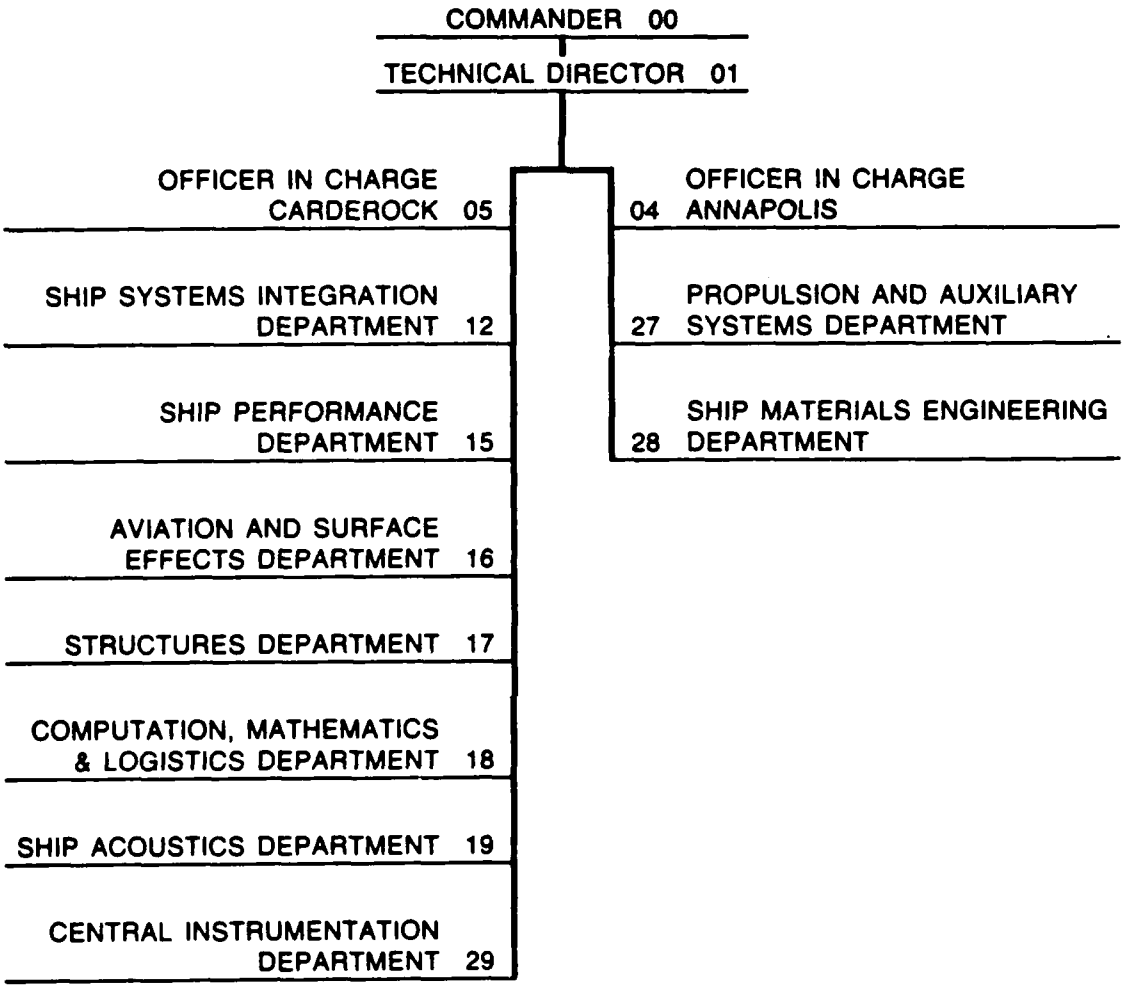

DESTRUCTION NOTICE — For **classified** documents, follow the procedures in DOD 5220.22M, Industrial Security Manual, Section II-9, or DOD 5200.1-R, Information Security Program Regulation, Chapter IX. For **unclassified**, limited documents, destroy by any method that will prevent disclosure of contents or reconstruction of the document.

ROUGHNESS EFFECTS ON

ITTC PROPELLER CAVITATION

by

Young T. Shen

Kirk J. Anderson

Approved for public release;
Distribution unlimited.

CONTENTS

FIGURES

TABLES

NTIS GRA&I
DTIC TAB
Unannounced
Justification
By
Distribution/
Availability Codes
Dist | Avail and/or Special
A-1

DTIC COPY INSPECTED

PHOTOS

ABSTRACT

Different cavitation patterns are often observed between the model propeller and the full scale prototype. Scale effects on cavitation inception and cavity extent cause uncertainty in the extrapolation of test results from model to full scale. The International Towing Tank Conference Cavitation Committee recognized this undesirable cavitation scaling problem and proposed an international cooperative program to investigate the use of leading edge roughness to reduce the cavitation scaling problem.

A 5-bladed bronze propeller was fabricated at MARIN (NSMB) in the Netherlands. The surfaces on blades 1 and 2 were smooth and the surfaces of blades 3 and 4 were sandblasted. Blade 5 was roughened with carborundum. The same propeller was tested in the facilities of the different committee members at the same loading conditions.

The model propeller was tested in the DTRC 24-Inch Variable Pressure Water Tunnel. The influences of Reynolds number, air content, various types of leading edge roughness, and blade loadings on cavitation were investigated. The cavitation test results were compared with the theoretically predicted pressure distribution to evaluate the effectiveness of using leading edge roughness in reducing the cavitation scaling problem.

ADMINISTRATIVE INFORMATION

This work was funded by the Naval Sea Systems Command under the Applied Hydromechanics Research Program, Element 61153N, Task Area R0230101 and was carried out by the Ship Hydromechanics Department under work units of 1542-817.

INTRODUCTION

It has often been assumed that cavitation inception occurs when the static pressure reaches the vapor pressure of the flowing fluid. This assumption is used in model cavitation tests and full scale predictions. The deficiency of this assumption is clearly brought out in the series of headform experiments organized by the International Towing Tank Conference (ITTC headform)[1]. The same model tested

at different facilities or the same facility at different test speeds and/or air contents showed different types of cavitation appearance and different indices of cavitation inception. Acosta and Parkin[1] pointed out that the free stream nuclei distribution and the boundary layer characteristics of the model are responsible for the chaotic appearance of cavitation patterns.

Field observations indicate that leading edge sheet cavitation occurs much easier on a full-scale propeller than on a model propeller at a given cavitation number. Experimental investigations clearly demonstrate that no leading edge sheet cavitation occurs if the boundary layer is laminar. This is the case in many model experiments. However, with a difference of two orders of magnitude in Reynolds number, the boundary layer is turbulent and leading edge cavitation occurs easily on a prototype propeller at high speeds[2]. Different cavitation patterns are often observed between the model and the prototype. Scale effects on cavitation inception and cavitation extent cause uncertainty in the extrapolation of test results from model to full scale. This fact contributes to one of the well known cavitation scaling problems.

Attempts have been made to improve model cavitation tests so that undesirable scale effects are reduced. Recent studies seem to indicate that distributed roughness around the leading edge of a foil can be used effectively to promote the onset of boundary layer transition either via the destabilization mechanism of the Tollemin-Schlichting waves at lower values of Reynolds numbers or via the mechanism of Strouhal oscillation at higher values of Reynolds number[3]. Uniformly distributed roughness or a single wire has been extensively used in aerodynamics and hydrodynamics to stimulate boundary layer development. A locally induced disturbance to the pressure and velocity fields around the leading edge by roughness elements should not significantly alter overall lift and drag characteristics, which are

of main interest for lifting surfaces in the absence of cavitation.

However, in marine applications the occurrence of cavitation is very sensitive to the magnitude of the local pressure field. The information accumulated on aerodynamics thus can not be used directly without going through a further refinement. This is evident from many recent publications on the subject of roughness distribution and cavitation[3,4,5].

The Cavitation Committee of the ITTC recognizes the potential benefit of applying distributed surface roughness to minimize the scale effect on leading edge sheet cavitation. In the 18th ITTC Cavitation Committee report, an international cooperative program was established to test the same model propeller in different facilities.

The objectives of this international cooperative program are as follows[6]:

1. To examine the effectiveness of leading edge roughness in reducing scale effects on cavitation inception.

2. To examine the condition of premature cavitation induced by the roughness elements and the subsequent influence on the cavity length.

3. To examine the effectiveness of leading edge roughness in decreasing the differences in cavitation inception and cavity extent between test facilities.

Because of the extreme sensitivity of cavitation to local propeller geometry, this program requires the use of identical propellers. The DTRC model propeller 4381 was designated by the 18th ITTC as the test propeller[7]. A brief description of this propeller geometry is given in Table 1. The ITTC model propeller was subsequently fabricated at MARIN (NSMB). This propeller has since been tested at MARIN[6], CSSRC (China)[8], and HSVA (Federal Republic of Germany)[9] and then shipped to DTRC. The cavitation tests described in the present report were conducted in DTRC's 24-inch variable pressure water tunnel. The first half of this test program focused on the test parameters recommended by the ITTC Committee. The second half of the

test program focused on the construction of cavitation inception buckets at several radial locations with different roughness distributions. The present report documents the results from the first half of the test program.

DESCRIPTION OF THE MODEL

The model is a five-bladed propeller with the expanded and projected outlines shown in Figure 1. This bronze model with a diameter of 250 mm was constructed at MARIN. The surfaces of Blades No. 1 and No. 2 are smooth. The surface of Blade No. 3 was sandblasted from the leading edge, the width of the sandblasted area varying with the blade radius. At 0.7 radius, the bandwidth is about 1.8 mm which is approximately 2.1 percent of the local chord length. Blade No. 4 was sandblasted in a strip at 1.5 mm from the leading edge with the strip width of 1mm. Blade No. 5 was carborundum coated from the leading edge. The width of the coated roughness is approximately 1.5 mm at 0.7 radius with a RMS roughness height of 0.093 mm. It is noticeable that the roughness on Blades 3, 4 and 5 cover both the back and the face of the blades. Photos 1a and b show the general view of roughness coverage at the outer radii. Photos 2a and b show the magnified view of the sandblasted patterns.

CAVITATION TEST RESULTS

Cavitation experiments were conducted in the open jet test section of the DTRC 24-inch variable pressure water tunnel. The propeller was mounted on the downstream shaft with an axially uniform inflow. To compensate for the tunnel wall effects on the flow field, the test speed in the water tunnel was set by using the thrust identity method based on open water data.

The open water data used in setting up the test conditions for the water tunnel were obtained in a towing tank. The measured K_T and K_Q values are given in Figure 2. For purposes of comparison, numerical computations were performed by using MIT's

PSF2 computer code. The friction coefficient used in the computation was based on a smooth blade surface. The computed results are plotted in Figure 2 along with the measured data. Good agreement between measured and computed K_T values is noted along with a slight difference in the K_Q data.

Three test conditions were set in the tunnel to reflect the influence of various types of propeller loading on cavitation.

Test Condition 1

The test conditions were $K_T = 0.18$ and $\sigma_n = 0.87$. At $K_T = 0.18$, the open water data give $J = 0.964$. The corresponding pressure distributions computed at several propeller radii from MIT's PSF2 computer code are shown in Figure 3. Lighthill's formula was used to correct the nonlinear effect around the leading edge. Within the resolution of this calculation no suction pressure peak is predicted at any blade radius, so that the blades experience shock-free entry. It is concluded that no leading edge sheet cavitation should occur at full scale with this type of pressure loading.

The cavitation patterns at this test condition are shown in Photo 3 at 1200 shaft RPM which gives a local Reynolds number of 1.12×10^6 at the 0.7 radius. Photo 3a shows the cavitation patterns for an air content of 40 percent of saturation at atmospheric pressure. First consider the cavitation pattern on Blade No. 1. Cavitation bubbles are visible at the inner radii from the root to 0.5 radius. In general, the photos indicate similar cavitation patterns on Blades No. 1 through 4. At this test condition, the influence of the sandblasting on cavitation seems negligible. However, Blade No. 5, which is coated with carborundum roughness, exhibits no cavitation bubbles. Previous experiments on a two dimensional hydrofoil showed that surface roughness reduces the effective camber and the pressure loading[10]. This may

explain the absence of cavitation bubbles on Blade No. 5.

To investigate the Reynolds number effect on cavitation, the shaft speed was increased to 2000 RPM which gives a local Reynolds number at 0.7 radius of 1.87×10^6. At the same air content of 40 percent of saturation at atmospheric pressure, the corresponding cavitation patterns are shown in Photo 3b. As pointed out by Kuiper, a propeller operated in a shock-free pressure distribution with a laminar boundary layer will show a number of bubble streaks when the Reynolds number is increased[4]. Photo 3b supports this. In addition to the cavitation bubbles, two spot cavities followed by continuous bubble streams are visible on Blade No. 2. The spot cavitation appears to be caused by flow transition induced by a leading-edge imperfection. The camera was not synchronized with the blade rotation so that no cavitation photo is available for Blade No. 1. As expected the number of cavitation spots on Blades 3 and 4 increased noticeably because of the sandblasted blade surface.

Once again, the cavitation pattern on Blade No. 5 is quite different from the others. At high speed the roughness elements induce cavitation right at the leading edge. This premature cavitation induced by the roughness elements at high Reynolds numbers has been discussed in Reference 10. The cavitation observation from Photos 3a and 3b suggest that the nominal roughness size used on Blade No. 5 is too coarse.

The air content was raised from 40 to 60 percent of saturation at atmospheric pressure to investigate the effect of postulated free-stream nuclei on cavitation. The test results at $R_e = 1.87 \times 10^6$ are shown in Photo 3c. It is observed from Photos 3b and 3c that the increase in air content not only increases the number of cavitation bubbles; it also increases the number of spot cavities on both the smooth and the rough blades. A slight increase in cavity length is also noted with the increased air content. As expected, bubble type cavitation is very sensitive to air content.

Theory predicts that cavitation will occur on a full scale propeller from the 0.4 to the 0.8 radius. The cavitation patterns on the sandblasted blades are in reasonably good agreement with the theoretical predictions when the model propeller was tested at high Reynolds number and high air content.

Test Condition 2

The tests were conducted at $K_T = 0.24$ and $\sigma_n = 1.03$. The open water data give $J = 0.84$ at $K_T = 0.24$. The corresponding pressure distributions and $-Cp_{min}$ computed at several radii are given in Figure 4 and Table 2. Weak suction pressure peaks occur around 3 to 5 percent of chord from the leading edge. A comparison of pressure distributions and the local cavitation numbers σ_ℓ as shown in Table 2 indicates that cavitation on a full scale propeller is expected to occur around the leading edge between the 0.4 to 0.8 radius. In the region between the 0.8 and 0.9 radii the computed $-Cp_{min}$ is only slightly lower than σ_ℓ. The difference is so small that cavitation could be expected to occur on the prototype because it is doubtful the surface would be smooth.

Test results at 1200 RPM and 40 percent air content saturation are shown in Photo 4a. The corresponding Reynolds number for this test condition is 1.10×10^6 at the 0.7 radius. In the case of the smooth blades, four streaks of cavities occur on Blade No. 1 from the 0.6 to 0.9 radii and three streaks on Blade No. 2 from the 0.7 to 0.9 radii. The number of streak cavities increases on the sandblasted or roughened blades, but the inner radii between 0.4 to 0.65 are still relatively free of cavitation.

With the shaft RPM increased to 1620 and air content maintained at 40 percent of saturation, Photo 4b shows the corresponding results. The Reynolds number at 0.7 radius at this test condition is 1.49×10^6. The blade area covered by cavities

increases noticeably with Reynolds number and surface roughness as seen in Photos 4a and 4b. However, even on the sandblasted blades there are still many bare spots between the cavities. It seems that a further increase in Reynolds number is needed to improve the cavitation coverage on sandblasted blades.

Cavitation covers all of Blade No. 5, however. Again, premature cavitation is induced by the carborundum roughness in the inner radii from the root to 0.4 radius and in the outer radii from 0.9 to the tip. Furthermore, the cavity lengths on Blade No. 5 are greater than the cavity lengths on the other blades at the same propeller radii. These problems might be avoided if the roughness size is reduced. This is the same recommendation given for Test Condition 1.

The air content was raise from 40 to 60 percent of saturation. The cavitation coverage is increased on Blades 1 and 2 and much increased on Blades 3 and 4 as shown in Photos 4c and 4d. The same conclusion given in Test Condition 1 is applicable to Test Condition 2. The agreement on cavitation patterns between predicted and measured is improved if the model is tested at high Reynolds number and high air content.

Test Condition 3

The tests were conducted at $K_T = 0.36$ and $\sigma_n = 2.37$. The open water data give $J = 0.63$ at $K_T = 0.36$. The corresponding pressure distributions and $-Cp_{min}$ computed at several radii are given in Figure 5 and Table 2. Very strong suction peaks are predicted in the outer radii. A comparison of computed pressures and the local cavitation numbers σ_ℓ indicates that leading edge sheet cavitation should occur at full scale from 0.45 radius to the tip.

Test results at 1200 RPM and 40 percent air content saturation are shown in Photos 5a. The corresponding Reynolds number at this condition is 1.06×10^6 at 0.7

radius. Cavitation patterns are almost identical on all five blades. Photos 5b and 5c respectively show the results when air content was raised to 60 percent of saturation and when the rotational speed was raised to 1620 RPM. In both cases the cavitation patterns on all blades are nearly the same.

Very strong suction peaks at the leading edge should occur at this test condition. The resultant negative pressure gradient may force the flow on a smooth blade to separate and reattach downstream. Hence a small separation bubble may form on a model propeller for which the Reynolds number is on the order of 10^6. (See References 11 and 12.) The photograph taken by Kuiper in his flow visualization work shows such a separation at a low value of J. (See Figure 2 of Reference 6.) Leading edge sheet cavitation forms easily when the boundary layer separates. It also forms easily when the boundary layer becomes turbulent with the surface roughness applied. Therefore, only minor differences in developed leading edge sheet cavitation are expected on model propeller blades with either a separation bubble or leading edge roughness. This explains why the Photos in 5a,b,c all look similar.

The boundary layer transition from laminar to turbulent should always take place right at the leading edge on a full scale propeller for which the Reynolds number is on the order of 10^8. Therefore, only minor scale effects on leading edge sheet cavitation are expected at heavily loaded operating conditions such as those in Test Condition 3, regardless of the blade condition.

CONCLUDING REMARKS

The theoretically computed pressure distributions from MIT-PSF2 code and Lighthill's leadind edge correction were used to evaluate the local pressure. With full-scale Reynolds number on the order 10^8, it is reasonable to assume that cavitation inception will occur on a prototype propeller if the local pressure on the

blade falls to or below the vapor pressure of the fluid.

At $K_T = 0.18$, the computed minimum negative pressure is at the midchord of the blade. The cavitation patterns observed on the smooth model blade surfaces are quite different from what the theory predicts. With the blade surface sandblasted, the agreement between observed and expected cavitation patterns is improved, at the high Reynolds number of 1.87×10^6 and high air content. The benefit of testing the model at high Reynolds number to minimize the cavitation scaling effect is reinforced by the present test results. The increase in air content promotes further development of cavities. The application of leading edge roughness with carborundum suppresses cavitation at low speed. Previous experiments on a two dimensional hydrofoil show that surface roughness reduces the effective camber and the pressure loading. However, premature cavitation induced by the roughness elements were visible at high speed. It is believed that a grain size of 0.093 mm is too big for this model propeller.

At $K_T = 0.24$, the propeller was almost operating at its design condition. The suction peak around the leading edge is so weak that the pressure loading is close to a roof-top shape. The boundary layer is laminar without separation on the smooth blades but is turbulent on roughened blades. The effectiveness of leading edge roughness to promote cavitation is clearly shown in the cavitation photos. However, the existence a of weak suction peak around the leading edge requires a careful selection of roughness size to avoid triggering premature cavitation.

At $K_T = 0.34$, the propeller was operating at an off-design condition. The computed pressure distributions show a strong suction peak right at the leading edge. The flow visualization work at MARIN indicated that the flow separated and reattached on the smooth blades to promote flow transition. Thus, no scale effect on cavitation was experienced at the extreme off-design condition. However, test

results from MARIN seem to suggest that there is still merit in using leading edge roughness to reduce the scale effect if the Reynolds number is not too large. Care should be exercised when selecting the proper location and roughness size to be applied.

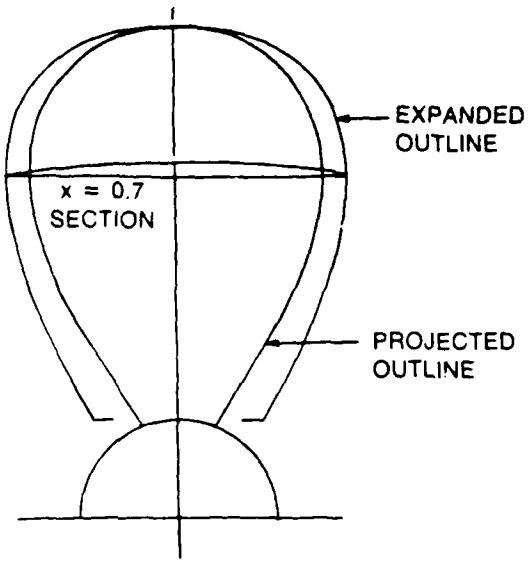

Fig. 1. Blade outlines of the model propeller 4381.

Table 1. Geometry of Propeller.

Number of blades	5
Expanded area ratio	0.725
Section meanline	NACA $a = 0.8$
Section thickness distribution	NACA 66 with NSRDC modified nose and tail
Design J	0.889
Design C_{Th}	0.5342

r/R	tan β_i	c/D	t/C	θ_s (deg)	P/D	f_M/c
0.2	1.8256	0.174	0.2494	0.0	1.2648	0.0311
0.3	1.3094	0.229	0.1562	0.0	1.3448	0.0368
0.4	1.0075	0.275	0.1068	0.0	1.3580	0.0348
0.5	1.8034	0.312	0.0768	0.0	1.3361	0.0307
0.6	0.6483	0.337	0.0566	0.0	1.2797	0.0245
0.7	0.5300	0.347	0.0421	0.0	1.2099	0.0191
0.8	0.4390	0.334	0.0314	0.0	1.1366	0.0148
0.9	0.3681	0.280	0.0239	0.0	1.0660	0.0123

Table 2. Local cavitation number versus computed $-C_{p\,min}$.

	J = 0.964, K_T = 0.18		J = 0.84, K_T = 0.24		J = 0.63, K_T = 0.34	
r/R	σ_ℓ	$-C_{p\,min}$	σ_ℓ	$-C_{p\,min}$	σ_ℓ	$-C_{p\,min}$
0.3	0.48	0.46	0.63	0.54	1.85	0.88
0.4	0.347	0.378	0.43	0.45	1.20	0.92
0.5	0.256	0.285	0.31	0.37	0.83	1.02
0.6	0.194	0.214	0.23	0.29	0.60	0.98
0.7	0.151	0.160	0.18	0.22	0.45	0.87
0.8	0.121	0.121	0.14	0.16	0.35	0.87
0.9	0.097	0.093	0.112	0.11	0.28	0.55

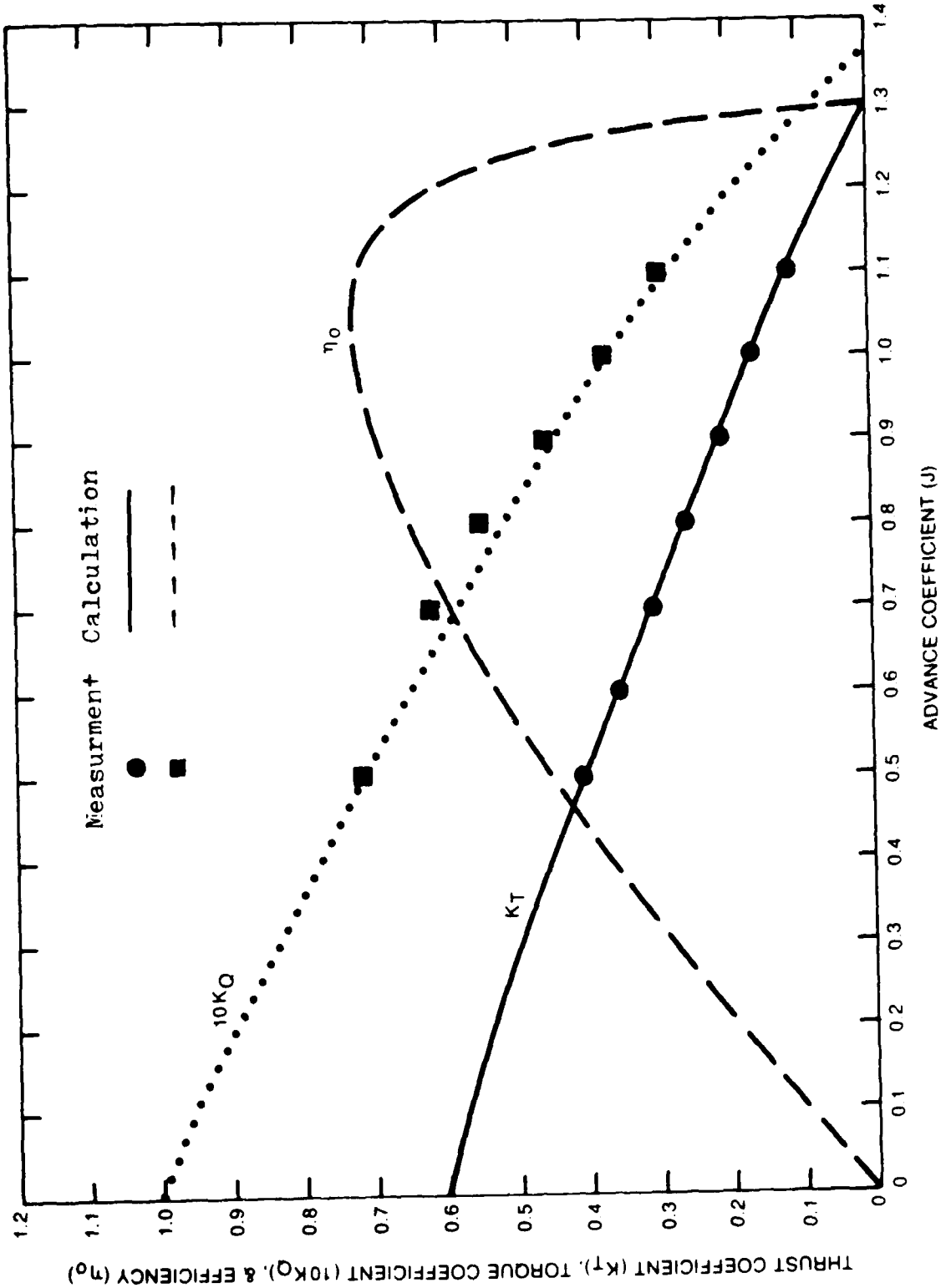

Fig. 2. Open water characteristics of ITTC propeller.

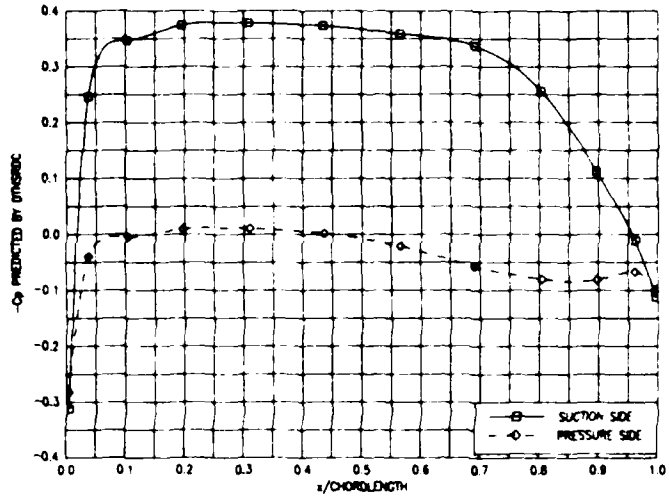

Fig. 3a. At the 40 percent radius.

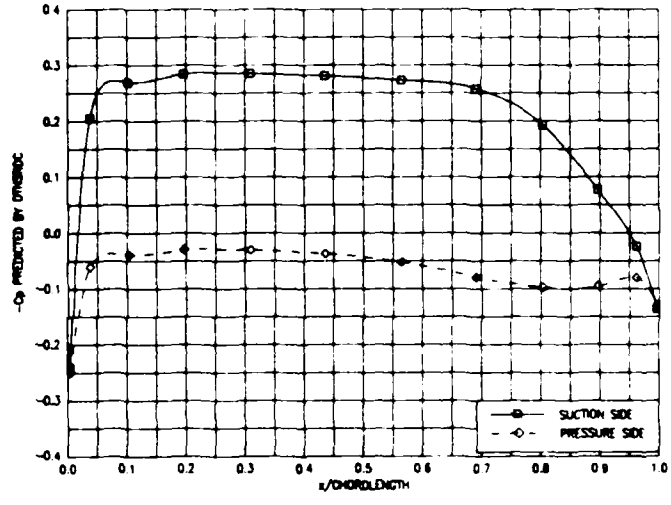

Fig. 3b. At the 50 percent radius.

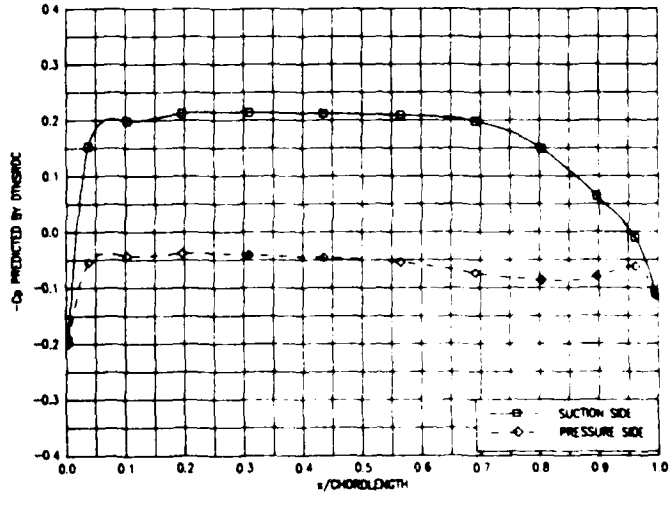

Fig. 3c. At the 60 percent radius.

Fig. 3. Predicted pressure distribution for J = 0.96.

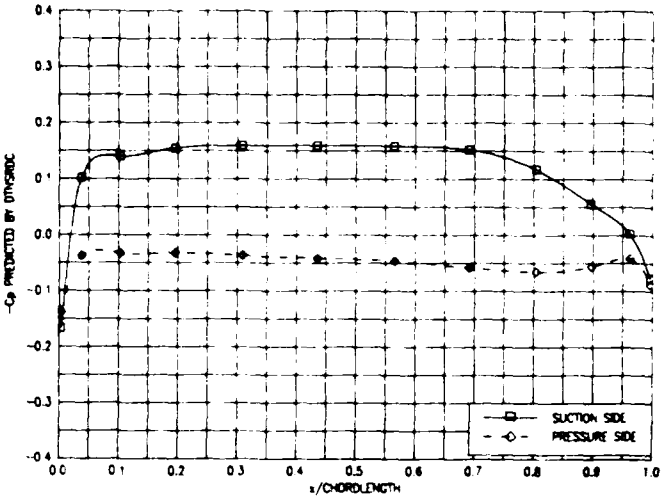

Fig. 3d. At the 70 percent radius.

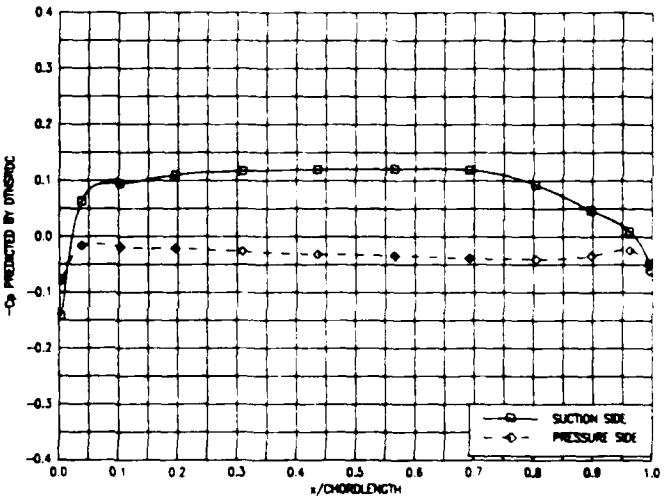

Fig. 3e. At the 80 percent radius.

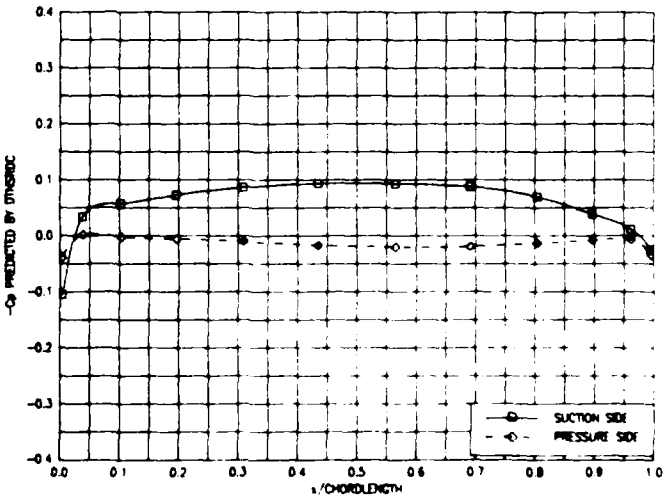

Fig. 3f. At the 90 percent radius.

Fig. 3. (Continued).

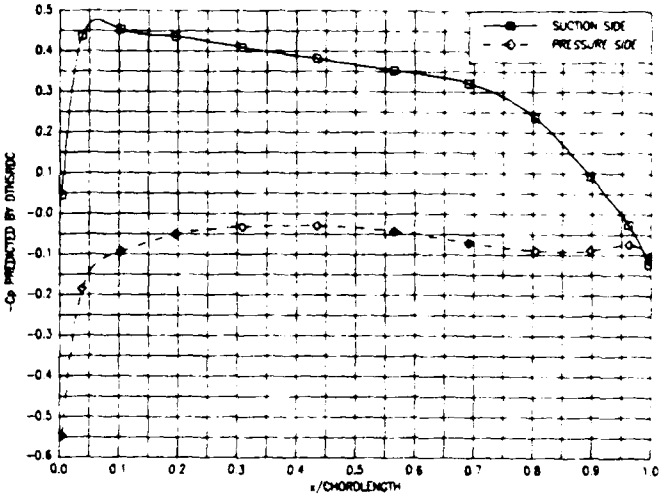

Fig. 4a. At the 40 percent radius.

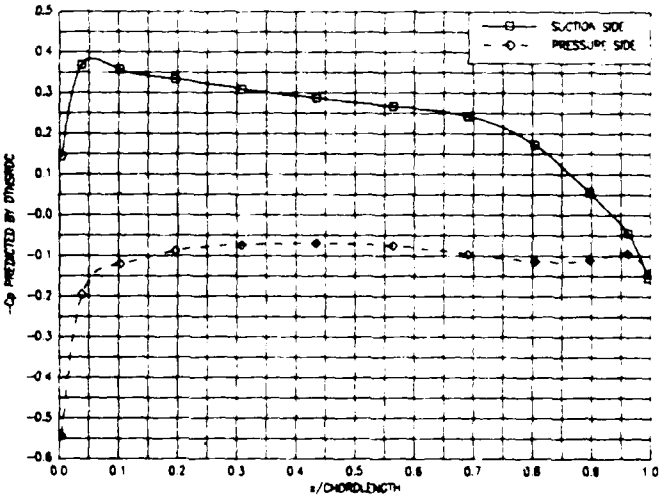

Fig. 4b. At the 50 percent radius.

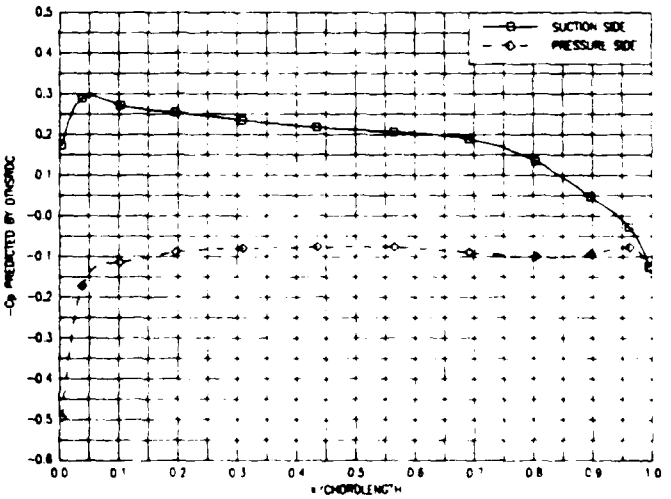

Fig. 4c. At the 60 percent radius.

Fig. 4. Predicted pressure distribution for J = 0.84.

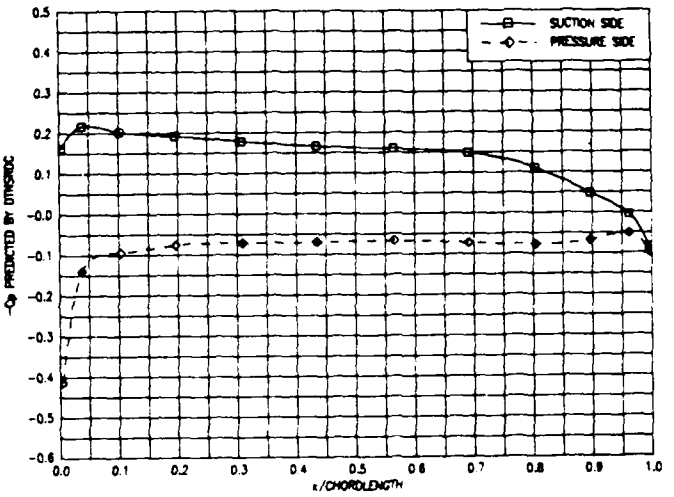

Fig. 4d. At the 70 percent radius.

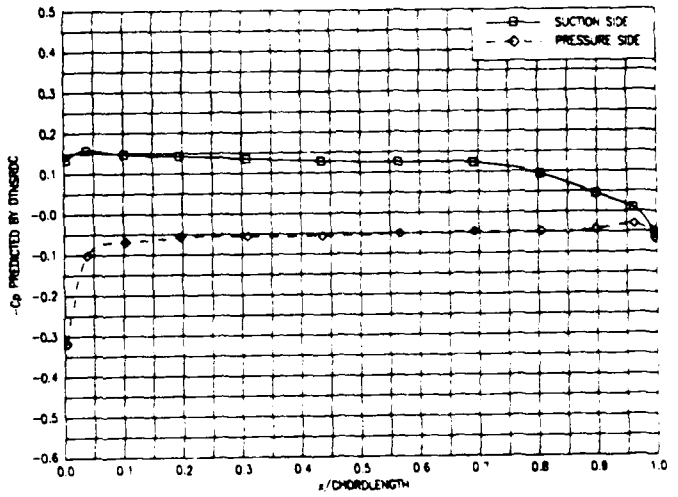

Fig. 4e. At the 80 percent radius.

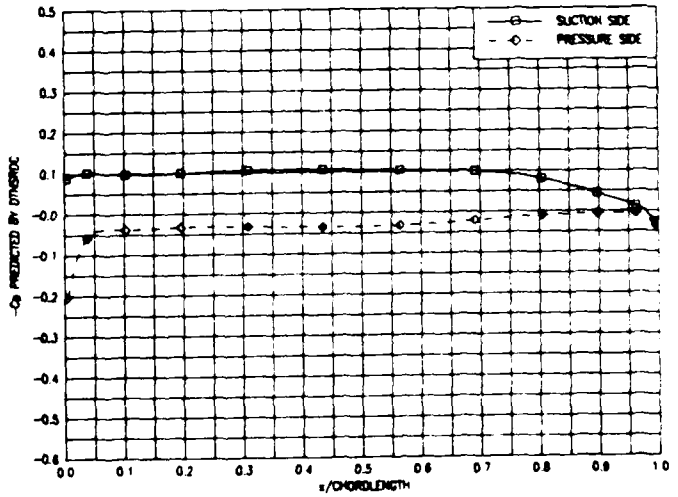

Fig. 4f. At the 90 percent radius.

Fig. 4. (Continued).

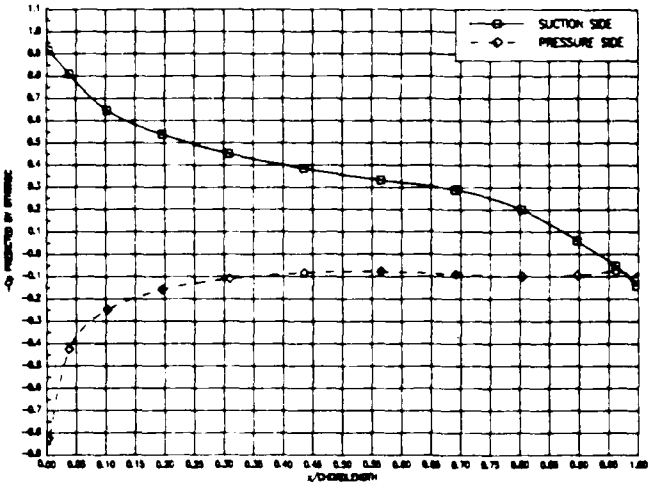

Fig. 5a. At the 40 percent radius.

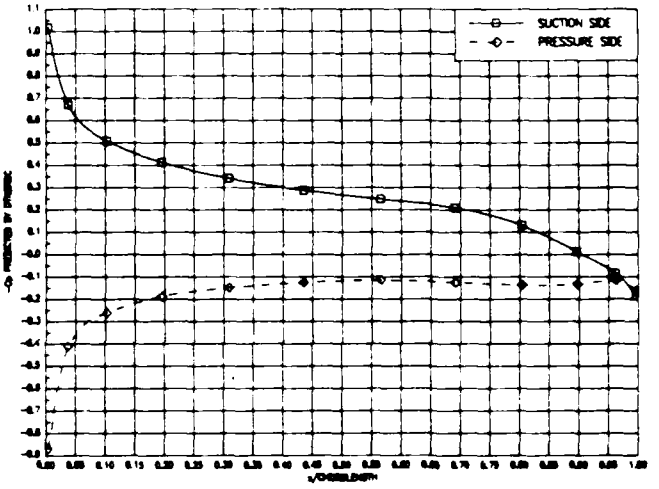

Fig. 5b. At the 50 percent radius.

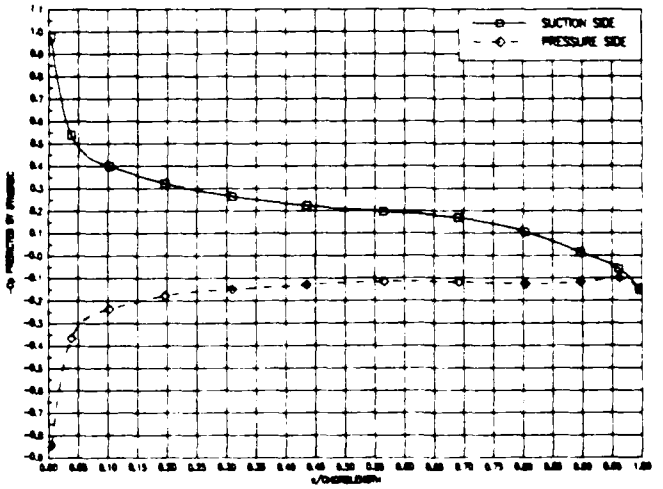

Fig. 5c. At the 60 percent radius.

Fig. 5. Predicted pressure distribution for J = 0.63

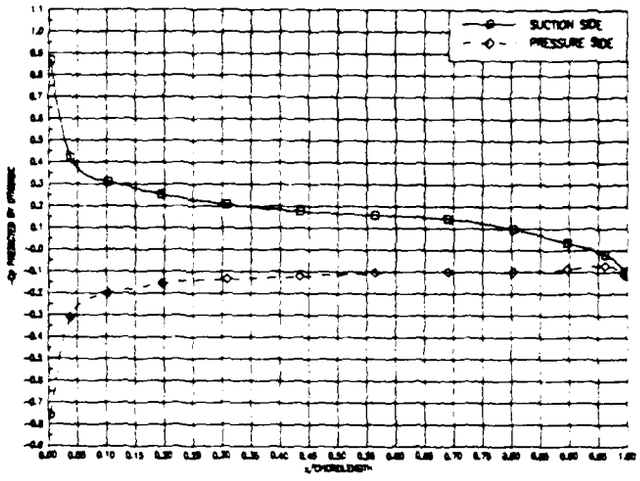

Fig. 5d. At the 70 percent radius.

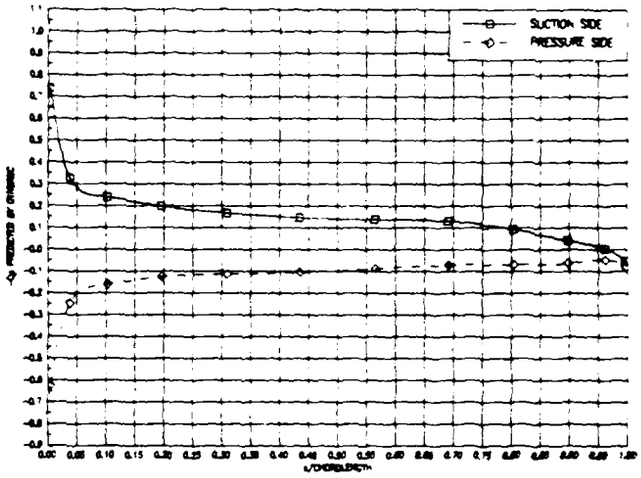

Fig. 5e. At the 80 percent radius.

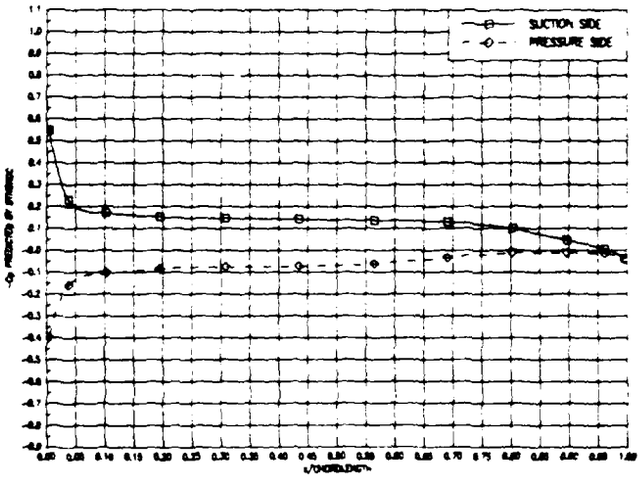

Fig. 5f. At the 90 percent radius.

Fig. 5. (Continued).

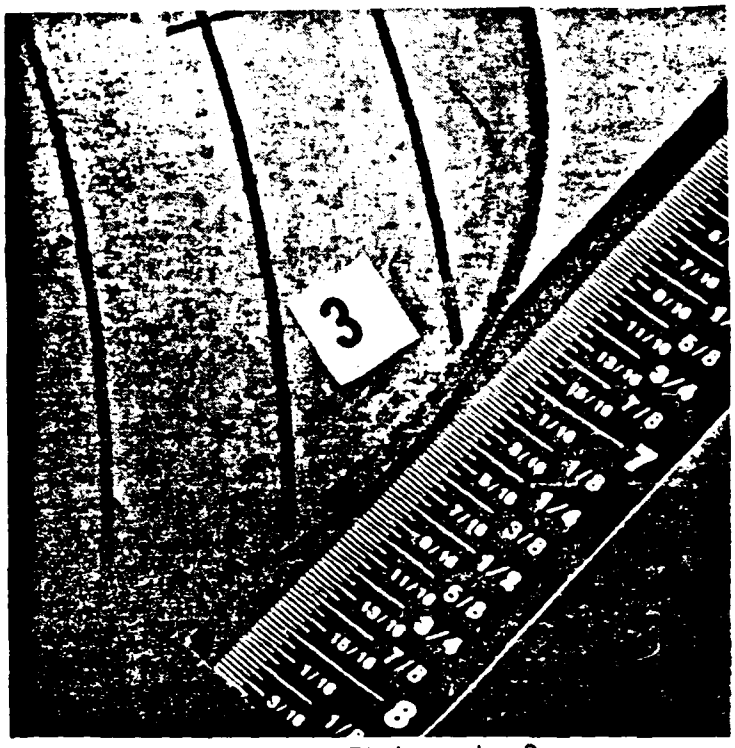

Photo 1a. Blade number 3.

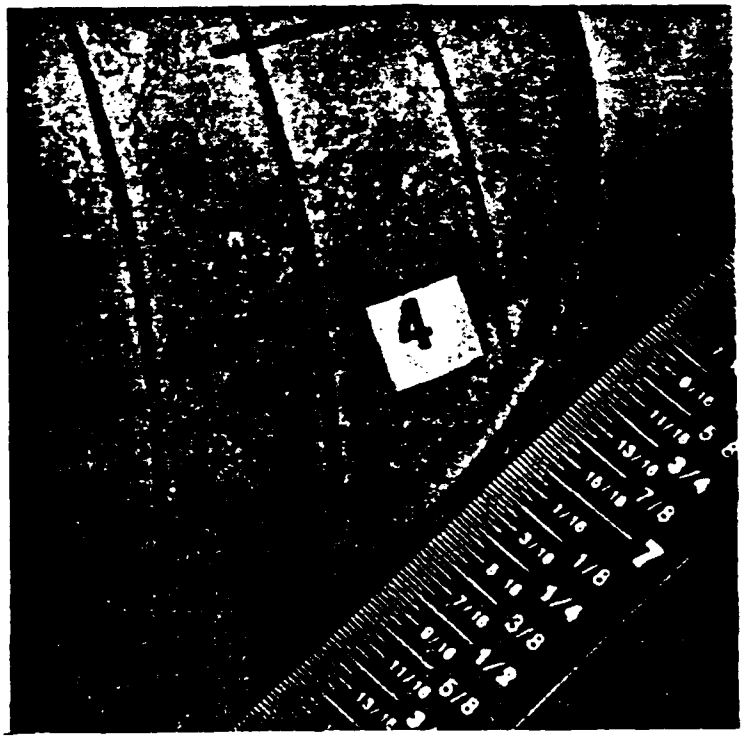

Photo 1b. Blade number 4.

Photo 1. Sandblasted blade surface.

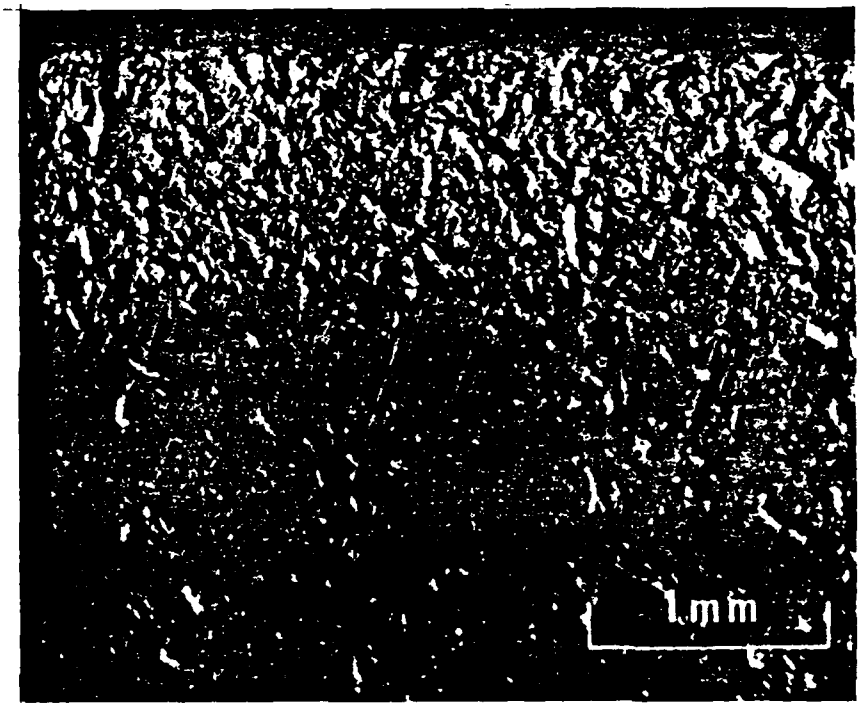

Photo 2a. Blade number 3.

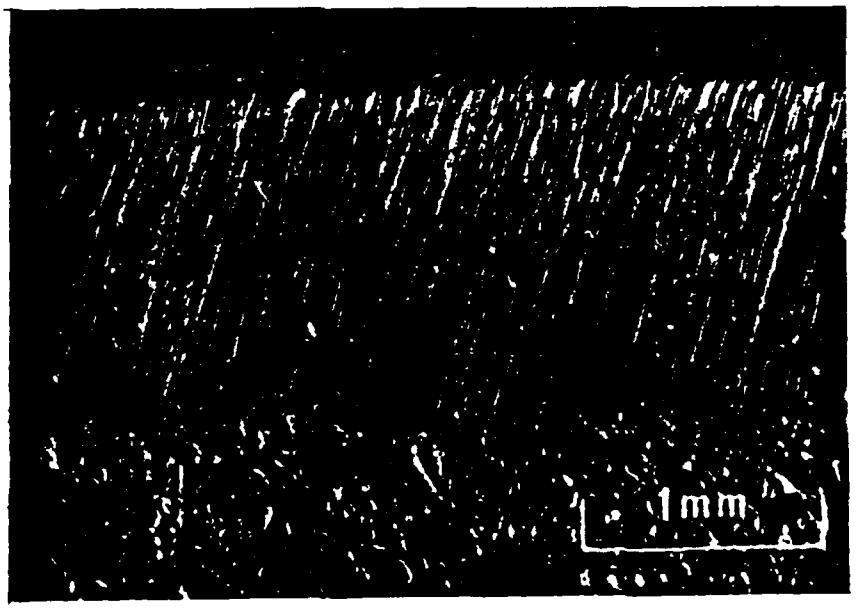

Photo 2b. Blade number 4.

Photo 2. Macro photographs of sandblasted regions (from ref. 6).

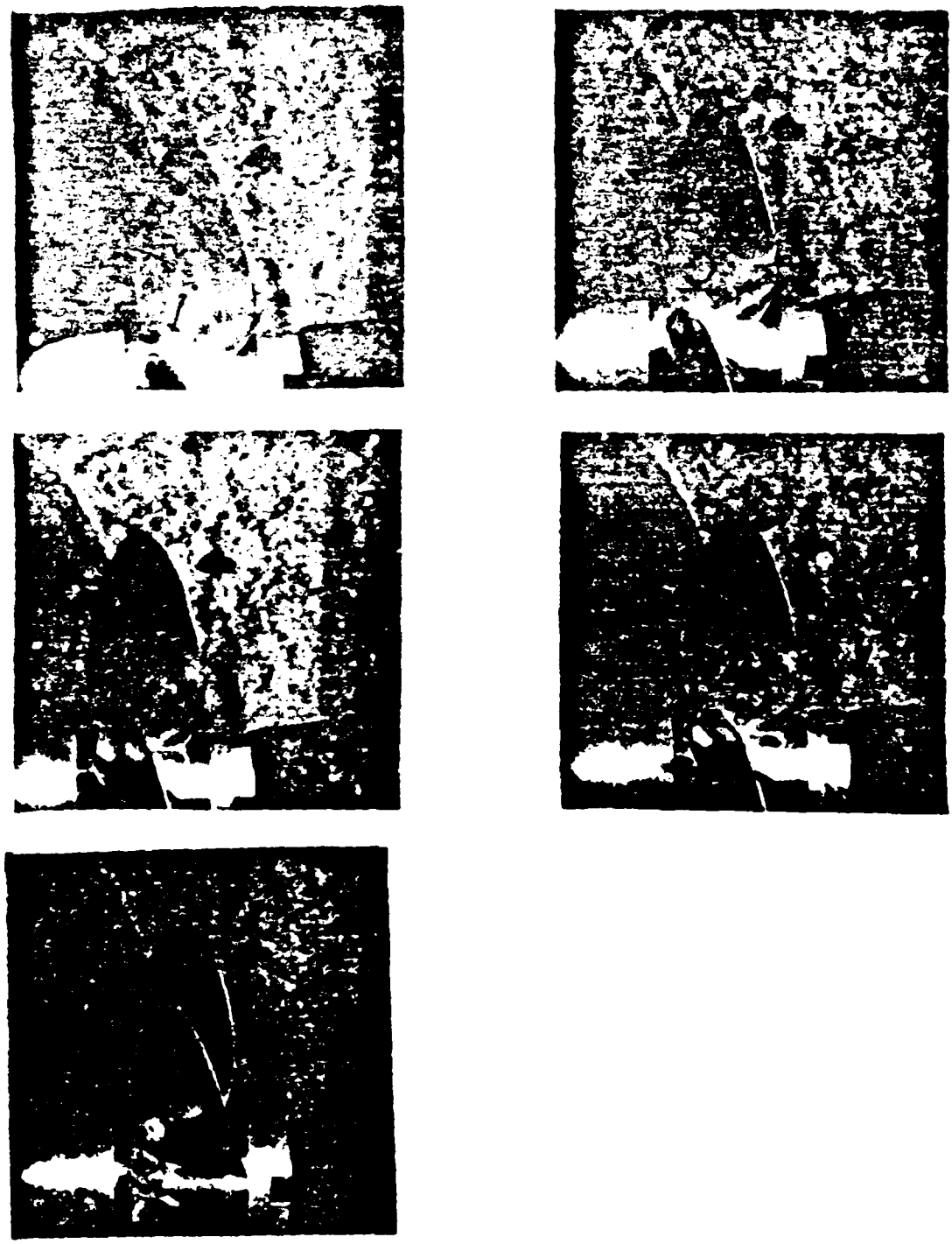

Photo 3a. n = 20 rps, air content = 40%

Photo 3. Cavitation patterns at test condition 1, K_T = 0.18 and σ_n = 0.87

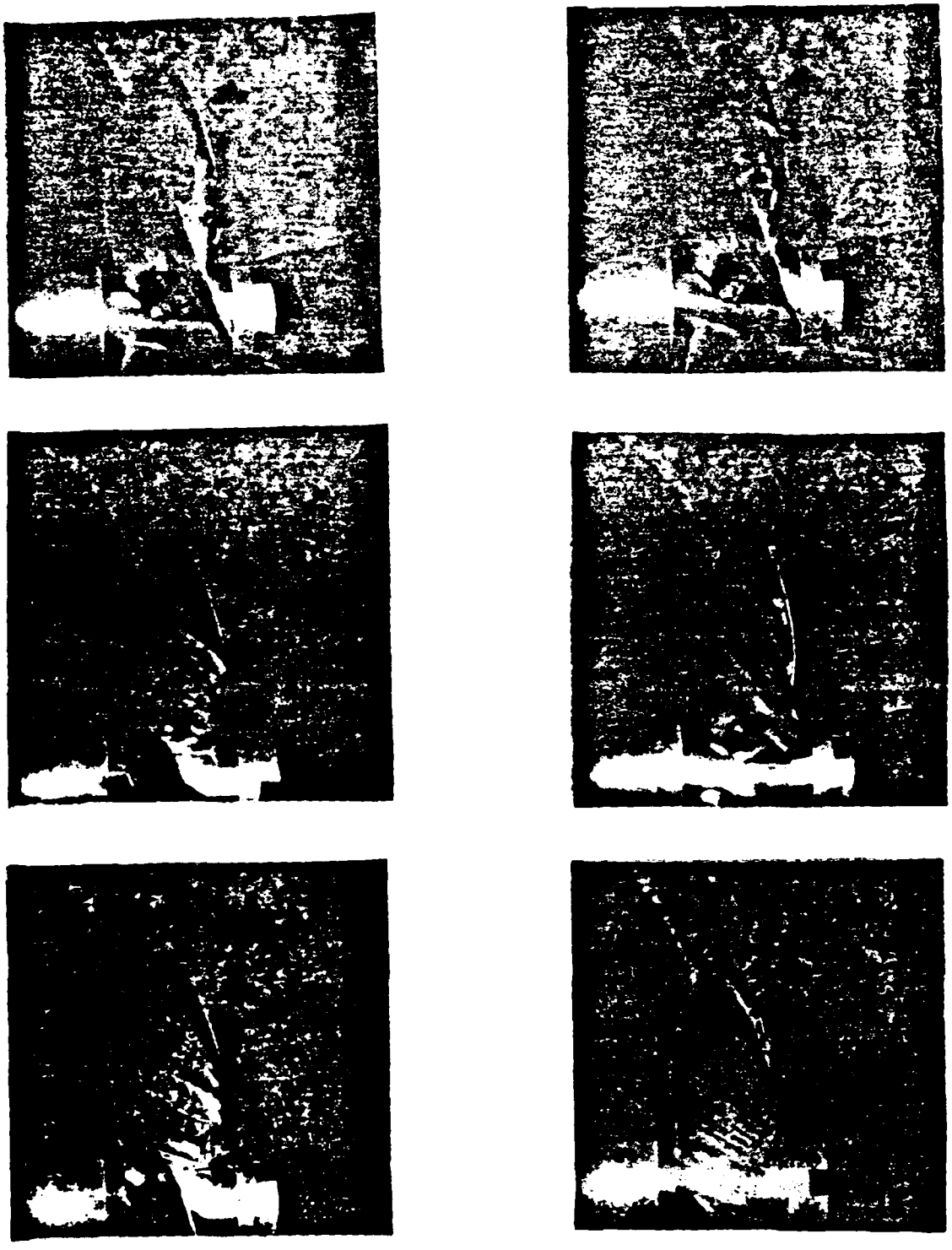

Photo 3b. n = 33.3 rps, air content = 40%.

Photo 3. (Continued).

Photo 3c. n ≈ 33.3 rps, air content = 60%.

Photo 3. (Continued)

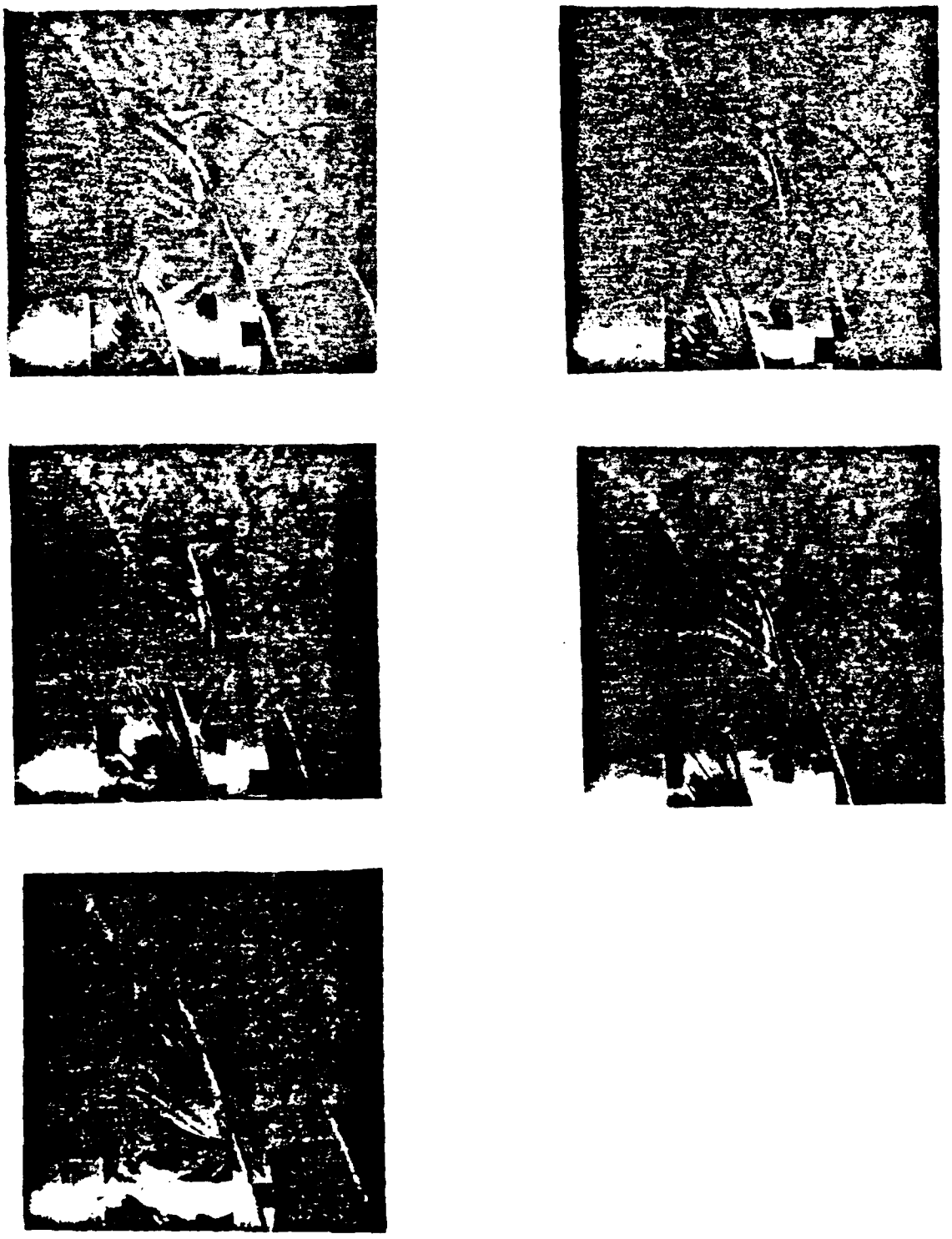

Photo 4a. n = 20 rps, air content = 40%.

Photo 4. Cavitation patterns at test condition 2, $K_T = 0.24$ and $\sigma_n = 1.03$

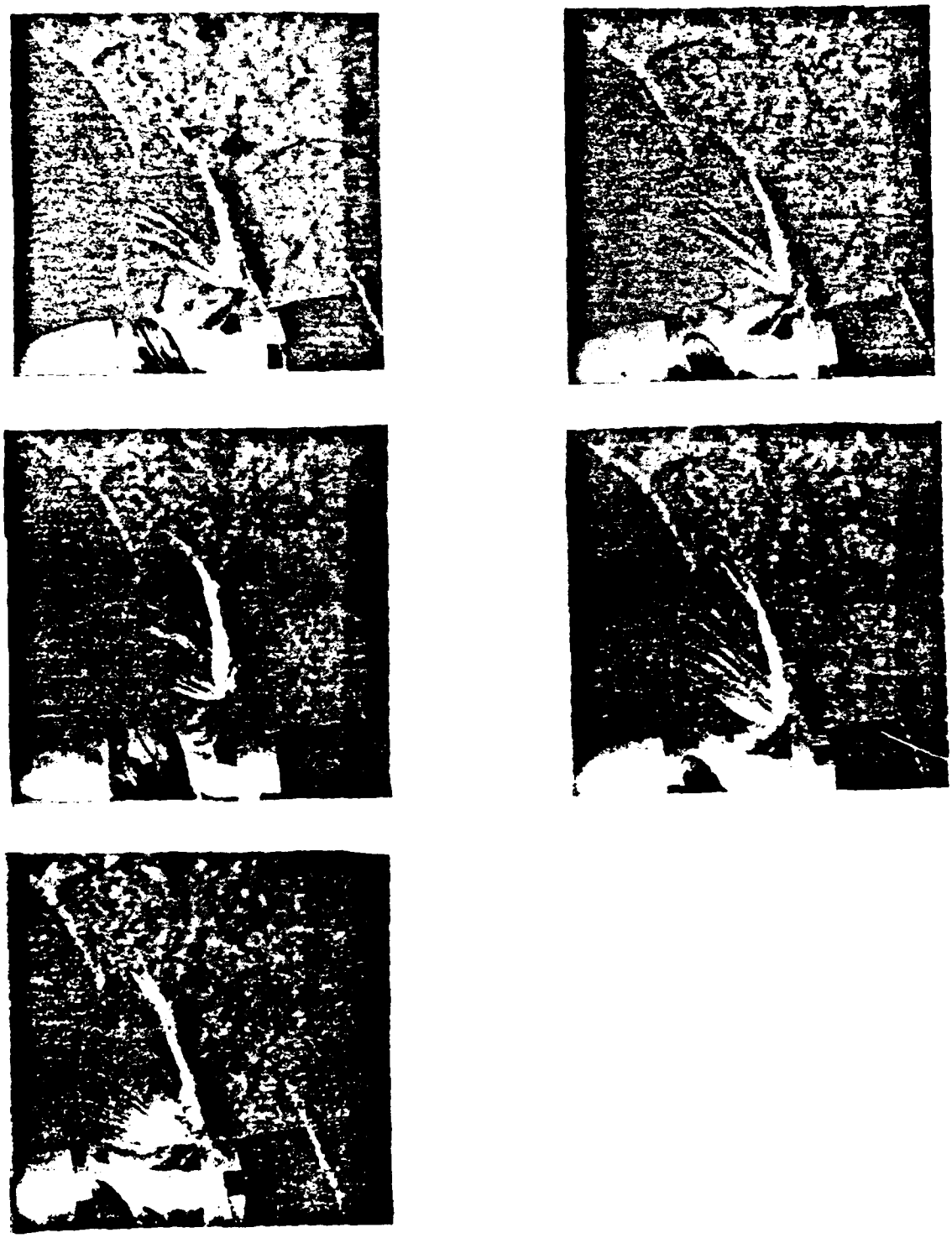

Photo 4b. n = 27 rps, air content = 40%.

Photo 4. (Continued)

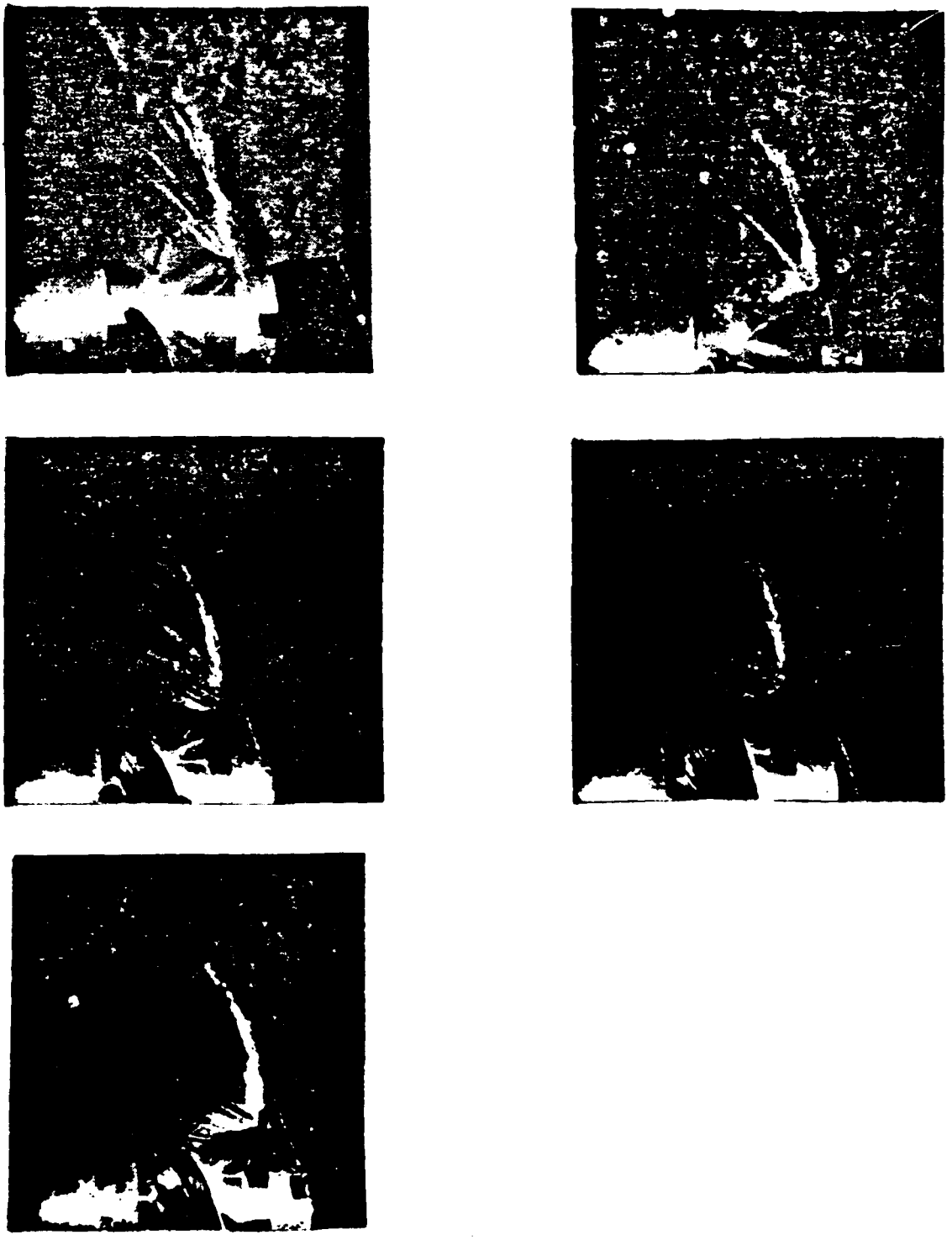

Photo 4c. n = 20 rps, air content = 60%.

Photo 4. (Continued).

Photo 4d. n = 27 rps. air content = 60°₀

Photo 4. (Continued)

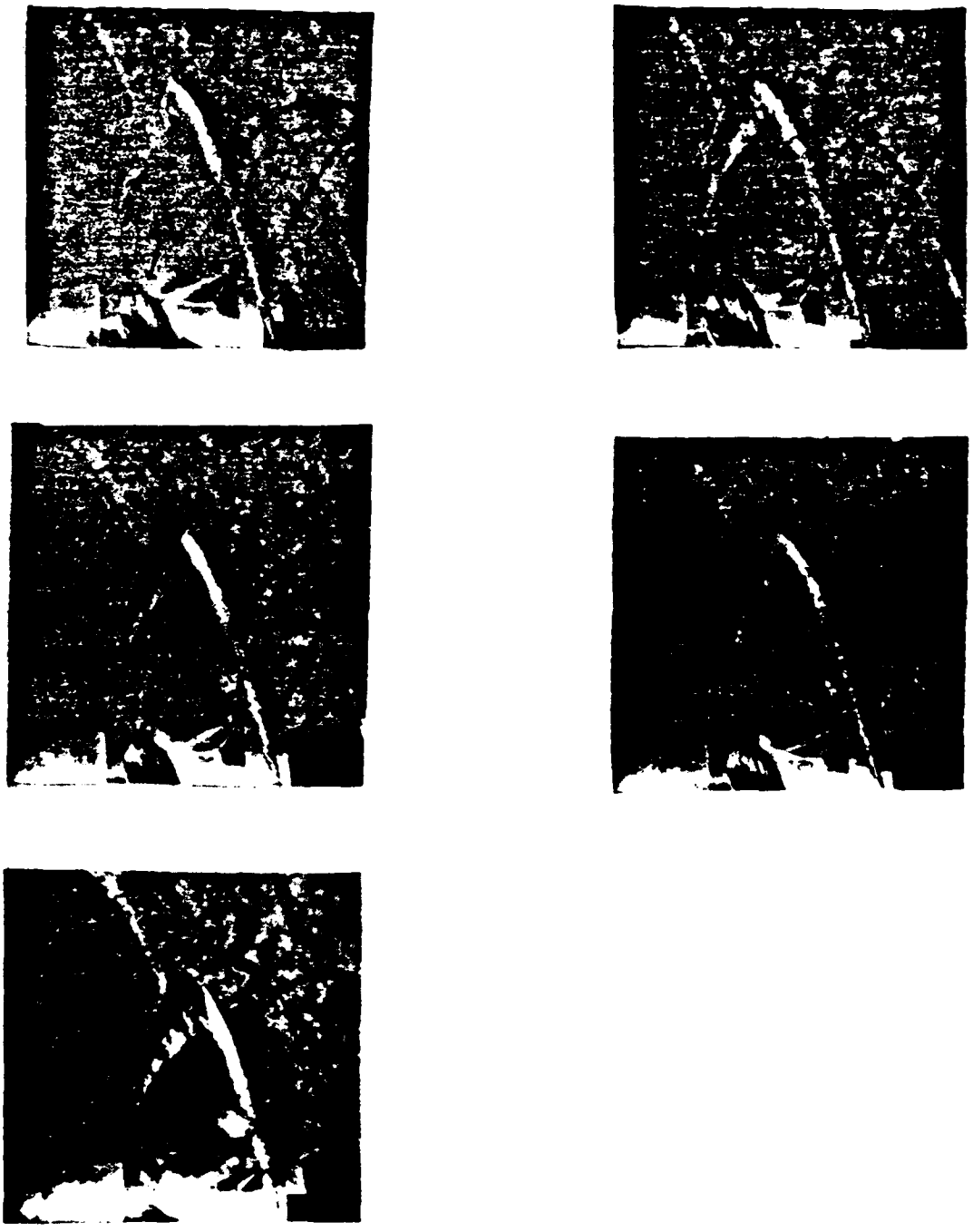

Photo 5a. n = 20 rps, air content = 40%.

Photo 5. Cavitation patterns at test condition 3, $K_T = 0.36$ and $\sigma_n = 2.37$.

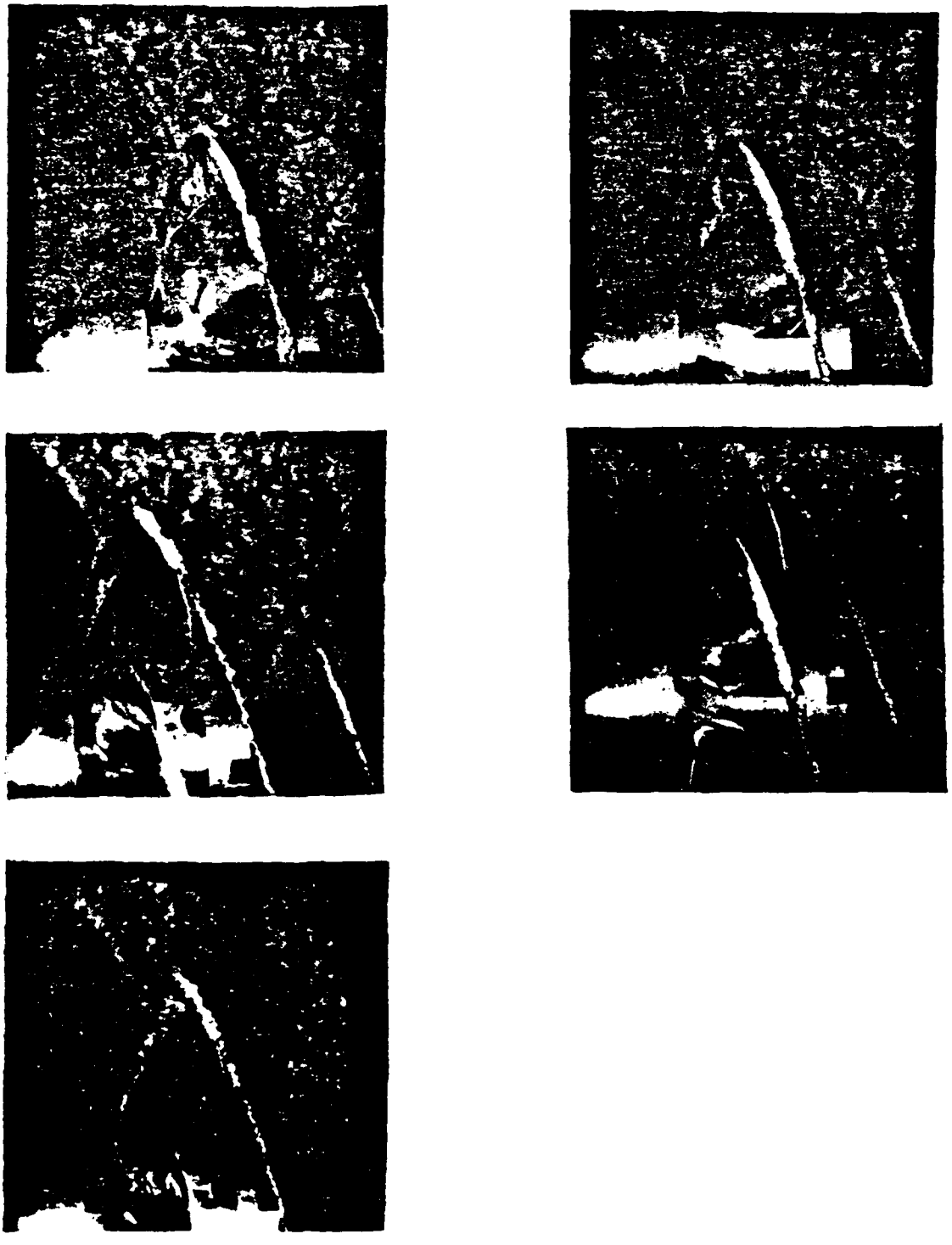

Photo 5b. n = 20 rps, air content = 60%.

Photo 5. (*Continued*).

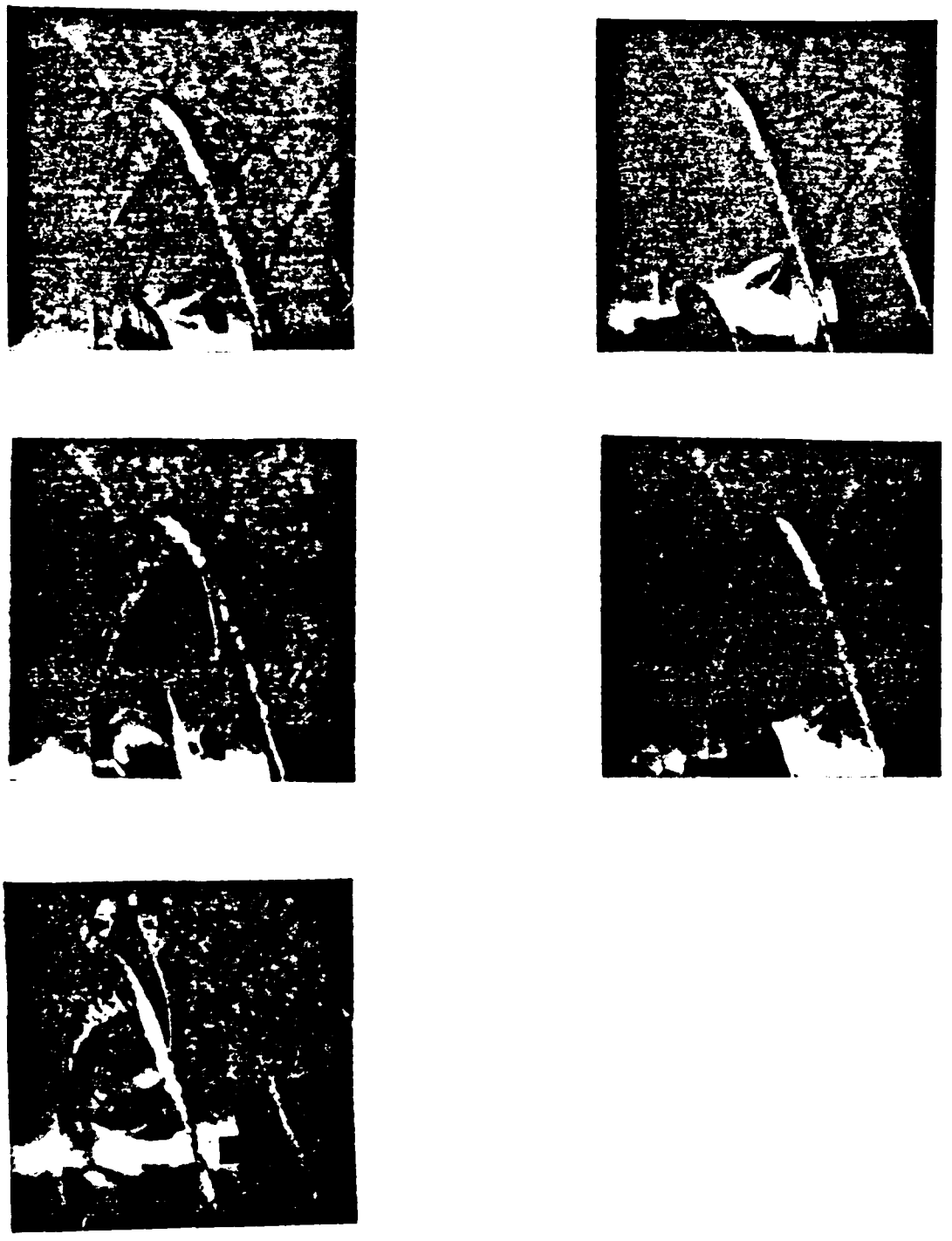

Photo 5c. n = 27 rps, air content = 60%.

Photo 5. (Continued).

REFERENCES

1. Acosta, A.J. and B.R. Parkin, "Cavitation Inception - A Selective Review," Journal of Ship Research, Vol. 19, No. 4, pp. 193-205 (1975).
2. Huang, T.T. and F.B. Peterson, "Influence of Viscous Effects on Model Full-Scale Cavitation Scaling," Journal of Ship Research, Vol. 20, No. 4, pp. 215-223 (1976).
3. Huang, T.T. and Y.T. Shen, "Application of Turbulence Stimulator to Reduce Scale Effect on Cavitation Inception," Proceedings of the International Symposium on Propeller and Cavitation, Wuxi, China (1986).
4. Kuiper, G., "Effects of Artificial Roughness on Sheet Cavitation," IMECH, pp. 151-166 (1983).
5. Ishii, N., H. Yagi, and H. Yuasa, "Model Testing of Propeller Cavitation by Roughening the Leading Edge of Blades," Journal of the Society of Naval Architects of Japan, Vol. 153, pp. 106-116 (1983).
6. Kuiper, G. "Recommended Test Conditions for ITTC Propeller with Leading Edge Roughness," NSMB Report No. 50618-1-RD (1986).
7. Boswell, R.J., "Design, Cavitation Performance, and Open-Water Performance of a Series of Research Skewed Propellers," DTNSRDC Report 3339 (1971).
8. Ye, Y.P. and T.K. Wang, "Cavitation Tests with the 18th ITTC Propeller Model No. 1 with Leading Edge Roughness," CSSRC Report 87004, Wuxi, China (1987).
9. Friesch, J., "Untersuchungen zum Einfluss von Aufrauhungen und der Propeller-kante auf die Kavitationserscheinungen," HSVA-Bericht 1549/86, Hamburg,Germany (1986).
10. Shen, Y.T., "Wing Sections for Hydrofoils - Part 3: Experimental Verifications," Journal of Ship Research, Vol. 29, pp. 39-50 (1985).

11. Kermeen, R.W., "Water Tunnel Tests of NACA 4412 and Walchner Profile 7 Hydrofoils in Noncavitating and Cavitating Flows," CIT Hydrodynamics Laboratory Report 47-5 (1956).

12. Katz, J., "Cavitation Phenomena Within Regions of Flow Separation," Journal of Fluid Mechanics, Vol. 140, pp. 397-436 (1981).

13. Parkin, B., "The Onset of Bubble-Ring Cavitation on Hemispherical Headforms," Journal of Fluids Engineering: ASME Vol. 104, pp. 115-122 (1982).

DTNSRDC ISSUES THREE TYPES OF REPORTS:

1. **DTNSRDC reports, a formal series,** contain information of permanent technical value. They carry a consecutive numerical identification regardless of their classification or the originating department.

2. **Departmental reports, a semiformal series,** contain information of a preliminary, temporary, or proprietary nature or of limited interest or significance. They carry a departmental alphanumerical identification.

3. **Technical memoranda, an informal series,** contain technical documentation of limited use and interest. They are primarily working papers intended for internal use. They carry an identifying number which indicates their type and the numerical code of the originating department. Any distribution outside DTNSRDC must be approved by the head of the originating department on a case-by-case basis.

END

DATE

FILMED

6-88

DTIC